Hindawi
International Journal of Zoology
Volume 2021, Article ID 5525109, 7 pages
https://doi.org/10.1155/2021/5525109

Research Article

Descriptive Study of Some Osteological Parts of Rosy Stone Lapper (*Garra rossica*) from Mashkid Basin of Iran

Mazaher Zamani-Faradonbe and Yazdan Keivany

Department of Natural Resources (Fisheries Division), Isfahan University of Technology, Isfahan 84156-83111, Iran

Correspondence should be addressed to Mazaher Zamani-Faradonbe; m.zamanif68@gmail.com

Received 28 January 2021; Revised 14 June 2021; Accepted 28 June 2021; Published 6 July 2021

Academic Editor: Joao Pedro Barreiros

Since osteological structures of fishes provide important biological and ecological information, studying these structures is valuable. On the other hand, due to lack of data on the osteology of stone lappers, the present study was conducted to provide detailed descriptive osteology of *Garra rossica* from Mashkid basin, southeastern Iran, comparing it with those of *G. typhlops* from the Bagh-e Loveh cave, Iran, *G. rossica* from Nahang River, Mashkid Basin, and *G. persica* from Zahak River, Sistan basin. For this purpose, 15 specimens of *G. rossica* were captured from Ladiz River, Mashkid Basin, using an electrofishing device, and fixed in 10% buffered formalin. Then, the specimens were cleared and stained with alcian blue and alizarin red for osteological investigations. A detailed description of the osteological features of *G. rossica* was provided. Based on the results, several differences were observed between the four species. *G. rossica* can be distinguished from *G. typhlops*, *G. persica*, and *G. rossica* based on the shape of suspensorium and opercular series, pharyngobranchial bones, ventral and pectoral girdles, caudal, dorsal, and anal fins skeleton, and shape and number of infraorbital elements.

1. Introduction

The cyprinid genus *Garra* Hamilton 1822 has a wide geographic distribution from Borneo, China, and southern Asia, through the Middle East, Arabian Peninsula, and East Africa to West Africa [1]. There are about 73 species in *Garra* [2], among which 14 species are recognized from Iran. Esmaeili et al. [3] listed four species *G. persica*, *G. rufa*, *G. variabilis*, and *G. rossica* [3]; recently, Sayyadzadeh et al. [4] reviewed the members of the genus in the Persian Gulf and Oman Sea basins and recognized six epigean species, including *G. barreimiae*, *G. longipinnis*, *G. persica*, *G. rossica*, *G. rufa*, and *G. variabilis*, and two subterranean species, including *G. typhlops* and *G. widdowsoni*, and described a new species from the region as *G. mondica*. Mousavi-Sabet and Eagderi [5] described a new species of *G. lorestanensis*. Esmaeili et al. [6] reviewed *Garra* genus species and introduced a new species, *G. amirhosseini*. Mousavi-Sabet et al. [7] described a new species of *G. roseae*. Moreover, Zamani-Faradonbe et al. [8] described *G. meymehensis* and *G. tiam*. Species of the genus *Garra* inhabit a wide range of substrates (muddy, sandy, and rocky bottoms) in streams, rivers, pools, and lakes [9]. They are primarily freshwater species but are also reported from brackish waters [1]. This genus is characterized by small-to-moderate body size and elongate and almost cylindrical body shape having a rounded snout with an inferior and crescent-shaped mouth, a horny lower jaw, usually fringed upper lip continuous with the snout, and a suctorial disc with a free posterior margin [2].

Despite the introduction of modern techniques such as DNA sequencing and barcoding, osteology, due to its reliability, still plays an important role in the systematic studies of fishes and comprises a major percent of today's works. Since osteological characteristics can provide valuable information in taxonomy and phylogenetic relationships of fishes [10], the present study was conducted to provide detailed descriptive osteology of *G. rossica* from the Ladiz River, Mashkid Basin, Iran.

2. Material and Method

Fifteen specimens of *G. rossica* were collected from Ladiz River, Mashkid Basin (total length: 60.77 ± 5.53 mm, mean ± SD) using the gill net and electrofishing device and

anesthetizing in 1% clove oil, then fixed in 10% buffered formalin, and transferred to the laboratory for further examinations. The specimens were cleared and stained with alizarin red S and alcian blue according to the protocol of Taylor and van Dyke [11] and Sone and Parenti [12] with some modifications for osteological examination. The cleared and stained specimens were studied using a stereomicroscope (Leybold Didactic GmbH model) and their skeletal elements were dissected and scanned by a scanner (HP Scanjet 3770) equipped with a glycerol bath. Drawing of the specimens was performed using CorelDraw X7 software. The terminology of skeletal elements follows Howes [13] and Rojo [14]. The detailed osteological features of *Garra typhlops* from the Tigris basin were provided by Jalili and Eagderi [15], *G. rossica* from Nahang River, Mashkid Basin, by Saemi-Komsari et al. [16], and *G. persica* from Zahak River, Sistan Basin, by Zamani-Faradonbe and Keivany [17].

3. Results

The ethmoid region of the neurocranium is flat and contains the kinethmoid, preethmoid-I, lateral ethmoid, supraethmoid, vomer, and nasal bones (Figure 1). The supraethmoid is broad and has two vertical and horizontal sections; the vertical section of this bone is located on the dorsal part of the vomer and the anterior part of the parasphenoid. The horizontal section bears two small anterior processes and a shallow middle depression with cartilaginous lateral margins (Figure 1). The posterior part of the vomer is pointed and overlapped with the anterior part of the parasphenoid and its anterior part has a V-shaped notch. The anterior part of the vomer is thicker than its posterior part. The ventral face of the vomer is smooth. The preethmoid-I bones are small and semicircular in shape and are present in the anterior-lateral edge of the vomer (Figure 1). The lateral ethmoid is located as a wall between the ethmoid and orbital regions; the lateral part of the lateral-ethmoid bears two anterior and posterior processes. A cylindrical kinethmoid exists between the maxillary bones (Figure 1).

The orbital region comprises the frontals, parasphenoid, ptersphenoids, orbitosphenoids, and circumorbital series. The frontal is a large bony element of the skull roof with a serrated anterior edge and bent ventrally; it bears a mid-lateral pointed process. The supraorbital canal is enclosed by the lateral margin of the frontal. The two orbitosphenoids are fused via their ventral process that is also connected to the parasphenoid (Figure 1). The ptersphenoid is concaved in shape with two ventral processes for connecting to the parasphenoid and bears two pores. The ptersphenoid is dorsally attached to the frontal, anteriorly to the orbitosphenoid, and posteriorly to the sphenotic. The anterior half of the parasphenoid is wider and is of typical shape with a serrated anterior rim and its posterior half has a triangular structure that its posterior margin bifurcates via a deep groove and has some pores in its middle part (Figure 1).

The otic region includes the parietal, epiotic, sphenotic, pterotic, and prootic bones. The parietal bone is almost square-shaped, and its posterior-lateral margin overlapped asymmetrically and laterally the dorsal part of the pterotic and epiotic bones. The epiotic is oval-shaped with a posterior process (Figure 1); it is situated between the pterotic and supraoccipital bones. The pterotic is a quarter-circle in shape (Figure 1) and its posterior-lateral part is well-developed and probably fused to the dermopterotic. The sphenotic bears a lateral process that connects the middle process of the frontal; this bone is ventrally attached to the prootic and posteriodorsally to the pterotic (Figure 1). The two prootics are connected to each other ventrally and to the parasphenoid dorsally by a descending process. This bone has two pores on its anterior part.

The occipital region is composed of the supraoccipital, exoccipital, and basioccipital. The supraoccipital is pentagon in shape and has a blade-shaped crest; its lateral part is connected to the epiotic. The exoccipital bears a large ventral foramen on its middle concave part. In the dorsal part of the basioccipital, there are a pointed pharyngeal process and a concaved masticatory plate pointing laterally. The pharyngeal process has a dorsal fossa and a ventromedial ridge (Figure 1).

The upper jaw is made up of the paired maxilla, premaxilla, and unpaired kinethmoid. The two maxillae are located at the dorsal side of the premaxilla; the anterior part of the maxillae is wider than the posterior part. A notch on the lateral edge of the maxillae is marked. The premaxilla is wide, L-shaped, and articulated with the maxillae and dentary and the kinethmoid bone is situated between the two maxillae (Figure 2(a)).

The lower jaw is composed of three bones, including the dentary, articular and retroarticular. The dentary is L-shaped, and its anterior edge is flat. The coronoid process situated on the dorsal middle part of the dentary is oriented posteriorly. The middle part of the articular is wide and its posterior part bears an articulatory facet. The triangular-shaped retroarticular is a small bone situated under the posterior part of the articular; the posterior part of the retroarticular is connected to the interopercle via the retroarticular-interopercle ligament. A small and elongated coronomeckelian is observed on the medial face of the articular (Figure 2(a)).

The suspensorium series is formed of the hyomandibular, ectopterygoid, endopterygoid, metapterygoid, symplectic, quadrate, and palatine (Figure 2(a)). The hyomandibular bone is almost triangular in shape: its dorsal part is wider and posterior part bears two protuberances; the ventral part of the hyomandibular is connected to the interhyal. This bone is articulated to the posterior part of the neurocranium with two hyomandibular articulatory condyles and to the opercle by opercular articulatory condyle. The ectopterygoid, endopterygoid, metapterygoid, symplectic, and quadrate form a bony complex connecting to the anterior part of the neurocranium via the palatine. A long symplectic is enclosed by the metapterygoid posteriorly, by the quadrate anteriorly and by the preopercle posteriorly. The anterior part of the palatine bears three processes and slightly deep depression for connecting to the vomer and preethmoid-I.

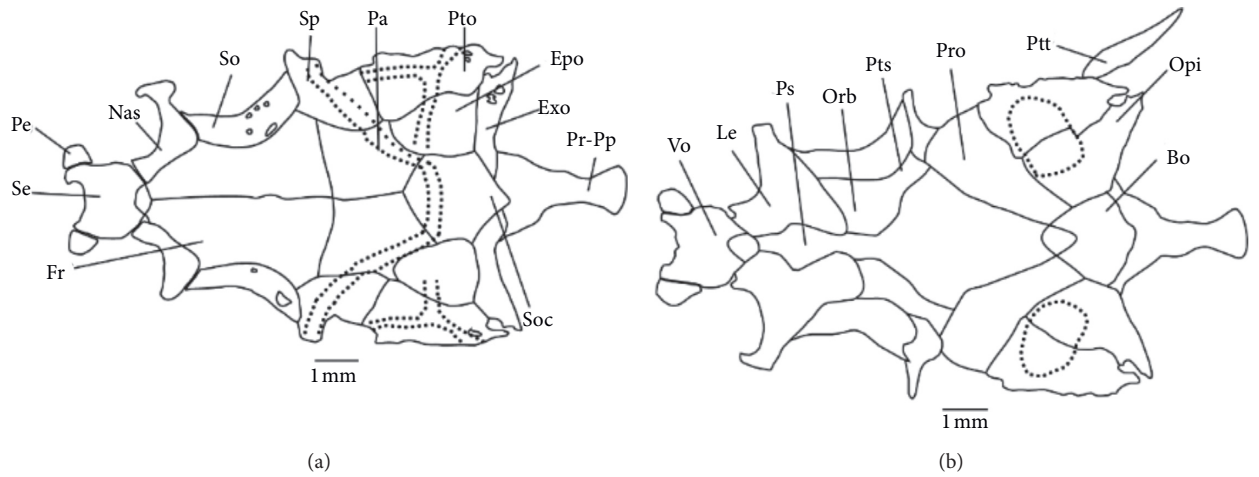

Figure 1: (a) Dorsal and (b) ventral views of the neurocranium in *G. rossica*. Bo: basioccipital; Epo: epiotic; Exo: exoccipital; Fr: frontal; Nas: nasal; Orb: orbitosphenoid; Pa: parietal; Pe: preethmoid-I; Ptt: posttemporal; Pr-Pp: posterior pharyngeal process; Pro: prootic; Ps: parasphenoid; Pts: pterosphenoid; Pto: pterotic; Se: supraethmoid; So: supraorbital; Soc: supraoccipital; Sp: sphenotic; Vo: vomer.

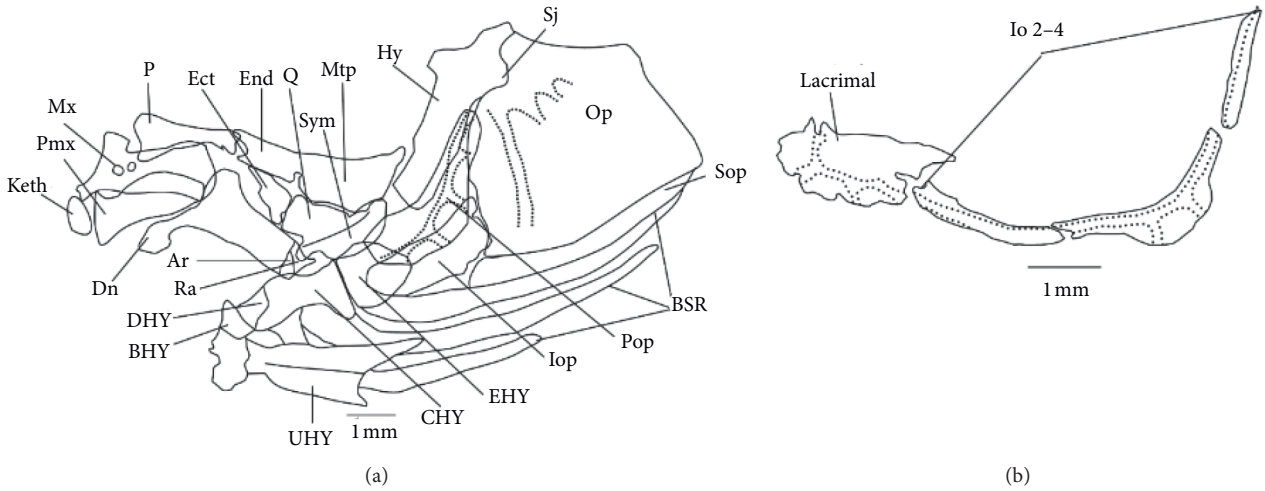

Figure 2: (a) The suspensorium, opercular series, and hyoid arch and (b) circumorbital series in *G. rossica*. Ar: articular; BBR: basibranchial; BHY: basihyal; BSR: branchiostegal; CBR: ceratobranchial; CHY: ceratohyale; DHY: dorsal hypohyal; EBR: epibranchial; Ect: ectopterygoid; End: endopterygoid; EHY: epihyal; HBR: hypobranchial; Hy: hyomandibulare; Io 2-4: infraorbital 2-4; Iop: interopercle; Keth: kinethmoid; Mx: maxillary; Mtp: metapterygoid; Op: opercle; P palatine; PBR: pharyngobranchial; Pmx: premaxillary; Pop: preopercle; Q quadrate; Ra: retroarticular; Sj: spine and socket joint; Sop: subopercle; Sym: symplectic; VHY: ventral hypohyal; UHY: urohyal.

The opercular series consists of four bones including the opercle, preopercle, subopercle, and interopercle bones. The opercle bone that is the largest element of this series has an opercular process in anterodorsal part and this bone has a socket joint that is connected to the hyomandibular. An L-shaped preopercle presents in the anterior side of the opercle and ventral side of the hyomandibular; its vertical part is longer than that of its wider horizontal part. The ventral part of the preopercle overlaps the dorsal part of the interopercle. The subopercle is long, and its anterior part is broad (Figure 2(a)).

The hyoid arch consists of the unpaired basihyal and urohyal and the paired epihyals, hypohyals, and ceratohyals and three pairs of branchiostegal rays. The urohyal is the largest element that has two vertical and horizontal sections. The posterior margin of its horizontal section is pointed and its middle part is wider. In addition, the anterior part of its horizontal section is branched. The posterior part of the ceratohyal is wider than its anterior part; its anterior part is branched and connected to the dorsal and ventral hypohyals. The dorsal and ventral hypohyals are fused. The basihyal is T-shaped, situated between the hypoyals (Figure 2(a)).

In the circumorbital series, the number of the infraorbital bones was the same in the studied specimens. There are four infraorbital and one supraorbital elements. The first circumorbital, i.e., lacryamal, is the largest element of this series. The supraorbital is oval-shaped and located at the lateral side of the frontal. The suborbital canal is enclosed by the infraorbital bony elements (Figure 2(b)).

The branchial apparatus includes five types of bones, including five pairs of the ceratobranchials, four pairs of the epibranchials, three pairs of the hypobranchial and two pairs of the pharyngobranchial, and three unpaired basibranchial. The fifth ceratobranchial is crescent in shape with a dental. There are three rows of pharyngeal teeth with a dental formula of 2.4.5-5.4.2 (Figure 3).

The dorsal fin bears one unbranched ray and nine branched rays, eight pterygiophores and one stay bone (Figure 4(a)). The first pterygiophore is the largest, U-shaped (bifurcates), and supports unbranched ray and first branched ray. The first pterygiophore is next to the 22th and 23th preural. A tetrangular stay bone supports the last branched ray. The anal fine originates at 12th preural. This fin has two unbranched and seven branched rays that were supported by six pterygiophores and one small stay bone (Figure 4(b)).

The caudal skeleton consists of the last centrum with the epural, parhypural, pleurostyle, uroneural, and six hypurals bones (Figure 5(c)). The pleurostyle is fused to the last centrum (urostyle). The neural arch of the second centrum is consumptive in some specimens. The first hypural is the largest one and attached to the parhyporal. The epural is a long bone positioning at the dorsal part of the neural arch of the first vertebra. There are 31–35 vertebra, including 15–17 cranial and 16–18 caudal centra.

The pectoral girdle consists of the cleithrum, coracoid, mesocoracoid, scapula, posttemporal, and radials (Figure 6(a)). The ventral part of the cleithrum is wider with a lateral process. This bone bears two wide horizontal and vertical portions; its ventral part bears an anteromedial downward process connecting to the anterior part of the coracoid. The posterior part of the coracoid is wider than its anterior part and bears an ascending process for connecting to the mesocoracoid. The posttemporal is a small bone that connects the pectoral girdle to the pterotic (Figure 1(b)). The medial part of the coracoid is bent ventrally and has a small pore. A semicircular scapula is located between cleithrum and coracoid bones; this bone bears a large foramen and is articulated to the first unbranched ray. The ventral part of the mesocoracoid is V-shaped and attached the coracoid to the cleithrum; the dorsal part of the mesocoracoid is broadened and attached to the medial surface of the cleithrum. The pectoral fin bears four radials; the lateral radial is the thickest and three others are long and flat.

Pelvic girdle includes the paired basipterygium, metapterygium, lateral pterygium, and radials (Figure 6(b)). The anterior part of the basipterygium bone is bifurcate; this bone has a posterior long and a midlateral processes. The two L-shaped lateral pterygiums are located at the posterolateral side of the pelvic bone. There are two paired radial and one paired metapterygium in the pelvic girdle.

4. Discussion

The present study provides a detailed skeletal description of rosy stone lapper (*G. rossica*) from Ladiz River, Mashkid Basin. Rosy stone lapper showed differences compared to *G. rossica* from Nahang River, Mashkid Basin, *G. persica* from Zahak River, Sistan Basin, and *G. typhlops*, a closely related species resulting from an evolutionary adaptation to a subterranean system. Most members of *Garra* genus are found in mountain streams and flowing waters [2], whereas *G. typhlops* inhabits subterranean habitats with stagnant waters [2].

There are differences in the suspensorium and opercular series, pharyngobranchial bones, ventral and pectoral girdles, caudal, dorsal, and anal fins skeleton, infraorbital series elements, and branchial apparatus between *G. rossica* of this study and *G. typhlops* provided by Jalili and Eagderi, [15], *G. rossica* from Nahang River provided by Saemi-Komsari et al. [16], *G. persica* from Zahak River, Sistan Basin, studied by Zamani-Faradonbe and Keivany [17]. All bones in suspensorium and opercular series in *G. rossica* are narrower and longer than *G. typhlops*. The pharyngobranchial bones in *G. rossica* are wide, while these bones are small in *G. typhlops*. *Garra rossica* has four infraorbital and one supraorbital elements, whereas these bones in *G. typhlops* had six infraorbital elements and in *G. rossica* from Nahang River had five.

The basipterygium in *G. rossica* is bifurcate and its posterior process is rounded, whereas in *G. typhlops*, the basipterygium is trifurcate and its posterior process is pointed. *Garra rossica* bears narrow and long cleithrum and coracoid bones in the pectoral girdle, whereas *G. typhlops* bears broad and wide bones.

The caudal skeleton in *G. rossica* has 6 hypural plates, long epural, and narrow and a long neural spin, whereas *G. typhlops* bears 7 hypural plates, a short epural, and neural spin. Furthermore, differences were observed between the osteological structures of the median unpaired fins of *G. rossica* and *G. typhlops*. The dorsal fin in *G. rossica* has one unbranched ray and nine branched rays and eight pterygiophores, whereas *G. typhlops* bears three unbranched and seven branched rays and nine pterygiophores; *G. rossica* from Nahang River had three unbranched ray and nine branched rays and eight pterygiophores and G. persica had two to three unbranched rays and eight to ten branched rays and nine pterygiophores.

The anal fin in *G. rossica* has two unbranched and seven branched rays and is supported by six pterygiophores and one small stay bone, while this fin in *G. typhlops* had two unbranched and six branched rays, seven pterygiophores and one stay bone, *G. rossica* from Nahang River had two unbranched and six branched rays and is supported by six pterygiophores and one small stay bone and one unbranched and one branched rays that were supported by six pterygiophores and one small stay bone in *G. persica*.

The branchial apparatus in *G. rossica* has five pairs of the ceratobranchials while *G. rossica* from Nahang River and *G. persica* had four pairs; *G. persica* had three pairs of pharyngobranchial, while *G. rossica* in this study has two pairs; there are three rows of the pharyngeal teeth with a formula of 2.4.5-5.4.2 in *G. rossica*, whereas the dental formula was 3.5.6-6.5.3 in *G. rossica* from Nahang River.

The osteological features of *G. rossica* can reflect changes in its composing structures with a new adaptation to mountain streams that can be described as evolutionary novelties that gradually accumulated as modified anatomical

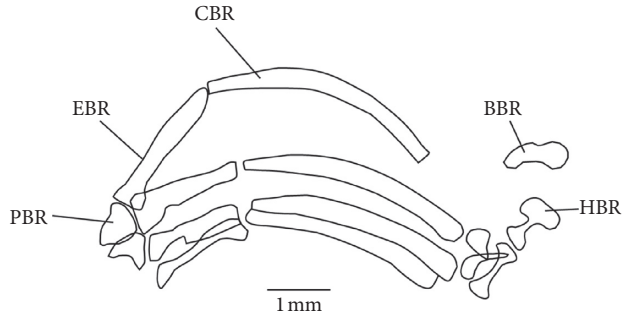

Figure 3: Branchial apparatus of *G. rossica*. BBR: basibranchial; CBR: ceratobranchial; EBR: epibranchial; HBR: hypobranchial; PBR: pharyngobranchial.

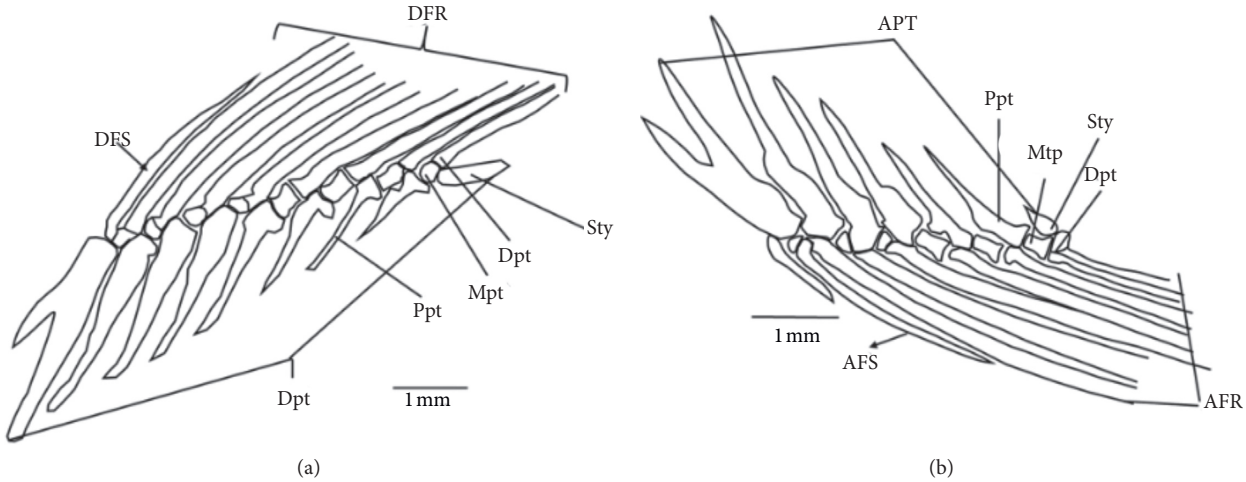

Figure 4: Lateral view of the (a) dorsal and (b) Anal fins of *G. rossica*. AFR: anal fin ray; AFS: anal fin spine; APT: anal pterigiophor; DFS: dorsal fin spine; DFR: dorsal fin ray; DPt: dorsal pterigiophor; Dpt: distal pterygiophore; Mpt: medial pterygiophore; Ppt: proximal pterygiophore; Sty: stay.

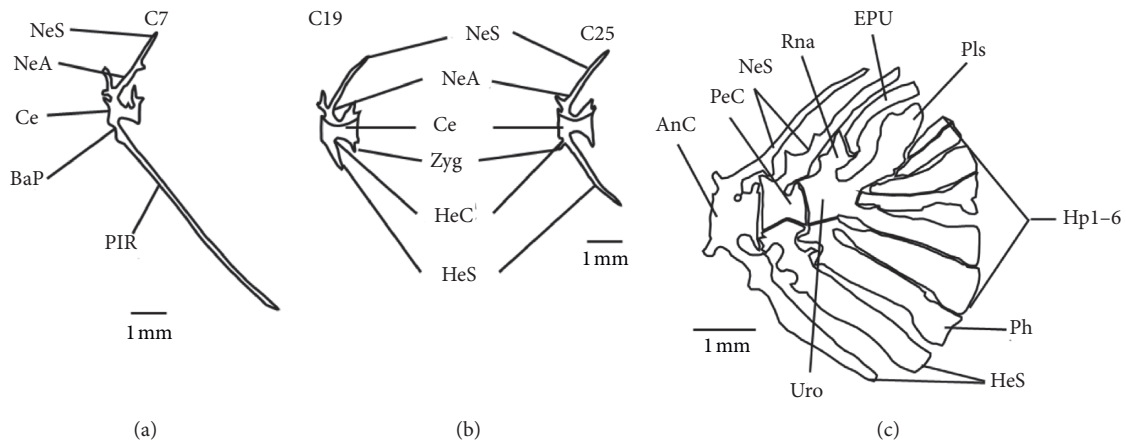

Figure 5: Lateral view of the (a) and (b) centrum 7, 19 and 25, (c) Caudal skeleton of *G. rossica*. Abbreviations: AnC: antepenultimate centrum; BaP: basapophysis; Ce: centrum; EPU: epural; HeC: hemal canal; HeS: hemal spine; Hp 1–6: hypural plates 1–6; NeA: neural arch; NeS: neural spine; PeC: penultimat centrum; Ph: parhypurale; PlR: pleural rib; Pls: pleurostyle; Rna: rudimentary neural arch; Uro: urostyle; Zyg: zygopophysis.

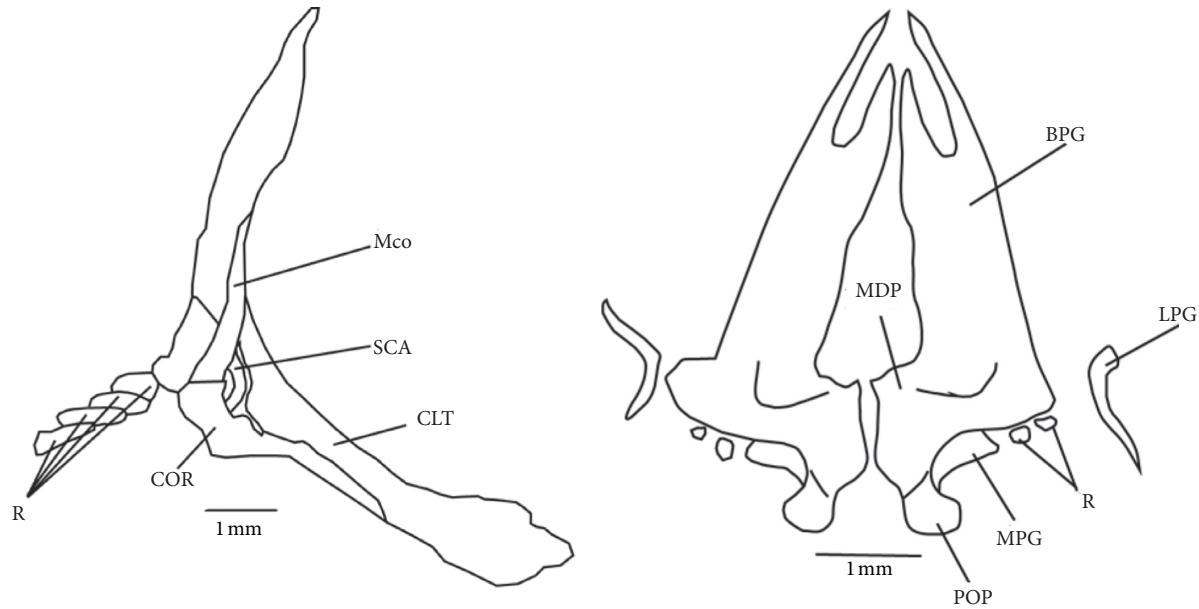

Figure 6: (a) Internal view of the pectoral girdle, and (b) ventral view of the pelvic girdle of *G. rossica*. BPG: basipterygium; CLT: cleithrum; COR: coracoid; LPG: lateral pterygium; Mco: mesocoracoid; MDP: medial process; MPG: metapterygium; POP: posterior process; R: radials; SCA: scapula.

structures as phenotypic plasticity during about 5 million years since it is divergent from their common ancestor with the other species in *Garra* genus.

Data Availability

All the data used for this study were obtained in the "Department of Natural Resources (Fisheries Division), Isfahan University of Technology" and are available for everyone.

Conflicts of Interest

The authors declare that they have no conflicts of interest.

References

[1] A. Getahun, "The american museum of natural history," Ph. D. thesis, Department of Anthropology, University of Colorado, Boulder, CO, USA, 1999.

[2] B. W. Coad, "Freshwater fishes of Iran," 2020, http://www.briancoad.com.

[3] H. R. Esmaeili, B. W. Coad, A. Gholamifard, N. Nazari, and A. Teimory, "Annotated checklist of the freshwater fishes of Iran," *Zoosystematica Rossica*, vol. 19, no. 2, pp. 361–386, 2010.

[4] G. Sayyadzadeh, H. R. Esmaeili, and J. Freyhof, "*Garra mondica*, a new species from the Mond River drainage with remarks on the genus *Garra* from the Persian Gulf basin in Iran (Teleostei: cyprinidae)," *Zootaxa*, vol. 4048, no. 1, pp. 075–089, 2015.

[5] H. Mousavi-Sabet and S. Eagderi, "*Garra lorestanensis*, a new cave fish from the Tigris river drainage with remarks on the subterranean fishes in Iran (Teleostei: cyprinidae)," *FishTaxa*, vol. 1, no. 1, pp. 45–54, 2016.

[6] H. R. Esmaeili, G. Sayyadzadeh, B. W. Coad, and S. Eagderi, "Review of the genus *Garra hamilton*, 1822 in Iran with description of a new species: a morpho-molecular approach (Teleostei: cyprinidae)," *Iranian Journal of Ichthyology*, vol. 3, no. 2, pp. 82–121, 2016.

[7] H. Mousavi-Sabet, M. Saemi-Komsari, I. Doadrio, and J. Freyhof, "Garra roseae, a new species from the Makran region in southern Iran (Teleostei: cyprinidae)," *Zootaxa*, vol. 4671, no. 2, pp. 223–239, 2019.

[8] M. Zamani-Faradonbe, Y. Keivany, S. Dorafshan, and E. Zhang, "Two new species of *Garra* (Teleostei: cyprinidae) from western Iran," *Ichthyological Exploration of Freshwaters*, no. 1137, pp. 1–22, 2021.

[9] M. Zamani-Faradonbe and Y. Keivany, "Biodiversity and distribution of *Garra* spp. (teleostei: cyprinidae) in Iran," *Iranian Journal of Fisheries Sciences*, vol. 20, 2021.

[10] Y. Keivany and J. S. Nelson, "Phylogenetic relationships of sticklebacks (Gasterosteidae), with emphasis on ninespine sticklebacks (*Pungitius* spp.)," *Behaviour*, vol. 141, no. 11, pp. 1485–1497, 2004.

[11] W. R. Taylor and G. C. Van Dyke, "Revised procedures for staining and clearing small fishes and other vertebrates for bone and cartilage study," *Cybium*, vol. 9, pp. 107–119, 1985.

[12] J. Sone and L. R. Parenti, "Clearing and staining whole fish specimens for simultaneous demonstration of Bone, cartilage, and nerves," *Copeia*, vol. 1995, pp. 114–118, 1995.

[13] G. J. Howes, "Anatomy and evolution of the jaws in the semiplotine carps with a review of the genus *cyprinion* heckel, 1843 (teleostei: cyprinidae) bulletin of the British museum (natural history)," *Zoology*, vol. 42, no. 4, pp. 299–335, 1982.

[14] A. L. Rojo, *Dictionary of Evolutionary Fish Osteology*, CRC Press, Boca Raton, FL, USA, 1991.

[15] P. Jalili and S. Eagderi, "Osteological description of Iran cave barb (*Iranocypris typhlops* Bruun & Kaiser, 1944)," *University Journal of Zoology, Rajshahi University*, vol. 33, pp. 01–07, 2014.

[16] M. Saemi-Komsari, H. Mousavi-Sabet, M. Sattari, S. Eagderi, S. Vatandoust, and I. Doadrio, "Descriptive osteology of *Garra rossica* (nikolskii, 1900)," *FishTaxa*, vol. 16, pp. 19–38, 2020.
[17] M. Zamani-Faradonbe and Y. Keivany, "Descriptive osteology of Persian stone lapper (*Garra persica*) from Sistan basin," *Journal of Animal Researches*, vol. 30, no. 3, pp. 346–357, 2018.